Preprint typeset in JHEP style - PAPER VERSION

Loop lessons from Wilson loops in $\mathcal{N} = 4$ supersymmetric Yang-Mills theory

Charalampos Anastasiou, Andrea Banfi

ETH Zurich, 8093 Zurich, Switzerland
E-mail: banfi@itp.phys.ethz.ch

Abstract: $\mathcal{N} = 4$ supersymmetric Yang-Mills theory exhibits a rather surprising duality of Wilson-loop vacuum expectation values and scattering amplitudes. In this paper, we investigate this correspondence at the diagram level. We find that one-loop triangles, one-loop boxes, and two-loop diagonal boxes can be cast as simple one- and two-parametric integrals over a single propagator in configuration space. We observe that the two-loop Wilson-loop "hard-diagram" corresponds to a four-loop hexagon Feynman diagram. Guided by the diagrammatic correspondence of the configuration-space propagator and loop Feynman diagrams, we derive Feynman parameterizations of complicated planar and non-planar Feynman diagrams which simplify their evaluation. For illustration, we compute numerically a four-loop hexagon scalar Feynman diagram.

Keywords: NLO Computations, Supersymmetric gauge theory, Extended Supersymmetry, Supersymmetry and Duality.

1. Introduction

$\mathcal{N} = 4$ supersymmetric Yang-Mills theory is rich of symmetries and surprising dualities. In the late 90s, Maldacena proposed that this conformal field theory in flat space-time is dual in its planar limit to a string theory in anti-de Sitter space [1]. Later investigations showed that anomalous dimensions of operators can be mapped to integrable quantum mechanical systems of spin-chains [2, 3, 4].

A surprising discovery was that the two-loop four-point planar amplitude could be expressed entirely in terms of the corresponding one-loop amplitude [5]. From the collinear limit of gauge theory amplitudes it was conjectured that this factorization may hold for all two-loop planar MHV amplitudes, while the AdS/CFT correspondence was inviting a general factorization at all orders in perturbation theory [5]. A factorization of the three-loop amplitude was proven in [6] where an explicit factorization ansatz valid at all orders was also formulated. Two-loop factorization was shown to hold for the five-point planar MHV amplitude [7, 8], however it was shown to break down for six-point scattering amplitudes [9].

Alday and Maldacena exploited the AdS/CFT correspondence to evaluate scattering amplitudes of $\mathcal{N} = 4$ supersymmetric Yang-Mills theory in the strong coupling limit, as a minimal surface on AdS_5 bounded by a polygon with sides the momenta of the external states [10]. This has lead to the conjecture that scattering amplitudes are dual to the vacuum expectation value of Wilson-loops order by order in perturbation theory [11, 12]. This duality has been tested with explicit comparisons at two loops for up to six-point amplitudes and hexagon Wilson loops [9, 13, 14].

The evaluation of Wilson-loop vacuum expectation values turns out to be much simpler than the corresponding two-loop amplitudes. Two-loop Wilson loops are known analytically up to hexagons [15, 16], and numerically for an arbitrary number of sides [17]. The relative simplicity of two-loop Wilson loops is due to that their Feynman representations require at most five integration variables irrespective of the number of the polygon sides. On the contrary, the number of Feynman parameters for an amplitude increases with the number of external legs.

$\mathcal{N} = 4$ supersymmetric Yang-Mills theory is rich of symmetries which constrain highly the structure of scattering amplitudes. The amplitude/Wilson-loop duality may be attributed to these symmetries. Nevertheless, these amplitudes require the computation of highly complicated scalar integrals which are typically the most complicated "master" integrals entering the evaluation of less symmetric amplitudes in theories such as QCD. For example, all four-point planar amplitudes in $\mathcal{N} = 4$ supersymmetric Yang-Mills through two loops are simple expressions in terms of the one-loop and two-loop box scalar (master) integrals [18, 19]. These very amplitudes being dual to a Wilson loop is not only a "magic" property of the theory but also a remarkable property of the one-loop box master integral.

In this paper we show that there is a correspondence between individual Wilson-loop diagrams and usual Feynman diagrams. We note that a scalar one-loop triangle is dual to a propagator of the Wilson-loop configuration space which joins a fixed point and a line segment. We also find that the one-loop box in six dimensions and the two-loop diagonal-

box in four dimensions with two light-like non-adjacent legs are dual to a configuration-space propagator joining two line segments.

An intriguing Wilson-loop two-loop diagram is the so called "hard diagram". It consists of a triple-gluon vertex connected via gluon propagators to three sides of a polygon Wilson-loop. An analytic solution for this diagram is fully known for square and pentagon Wilson loops [11, 20] while it is known in Regge kinematics[1] for a hexagon Wilson-loop [15, 16] and for an octagon in special kinematic configurations [21]. The "hard diagram" has only been computed numerically with standard methods for polygon Wilson loops with more than six sides [17]. In this paper, we demonstrate that the Wilson-loop "hard diagram" is dual to a four-loop hexagon diagram with four one-loop triangle subgraphs. We also derive a representation of the propagator in configuration space connecting a fixed point and a line segment as the product of two massive propagators. With this representation, we find that the "hard diagram" is dual to a one-loop hexagon massive Feynman integral integrated over its own mass parameters.

We hope that these representations of the "hard diagram" with an arbitrary number of polygon sides will become a convenient starting point for an analytic evaluation of it in the future. However, this and other two-loop Wilson-loop diagrams are relatively easy to evaluate numerically [17]. We can then exploit the diagrammatic dualities of Wilson loops and amplitudes to facilitate the computation of complicated Feynman integrals in amplitudes. For illustration, we present here a numerical evaluation of a scalar four-loop hexagon integral with light-like legs which is mapped to a scalar hexagon Wilson-loop "hard diagram" times a $1/\epsilon^3$ prefactor.

Inspired by the diagrammatic dualities we have found, we can derive simple representations for multi-loop integrals with "easy-box" subgraphs (boxes with two non-adjacent light-like legs). These are non-planar diagrams which are rather cumbersome to evaluate naively. We replace "easy-box" subgraphs by a single propagator reducing the number of loops by one. All two-loop non-planar integrals with such a subgraph are reduced to one-loop integrals where two of the external momenta are variables constructed as linear combinations of the only two external momenta entering the "easy-box" subgraph. A two-fold integration is also required over a range of such linear combinations for the external momenta. These representations require a smaller number of integration variables than canonical Feynman parameterizations. They also lead to simple Mellin-Barnes representations.

Our article is organized as follows. In Section 2 we derive the correspondence between a one-loop triangle and a propagator in configuration space. In Section 3 this correspondence is exploited to rewrite planar easy boxes as a configuration-space propagator joining two line segments. In Section 4 we consider the "hard diagram" contribution to a two-loop Wilson loop and show that it can be mapped into a four-loop hexagon. This correspondence is then used for a numerical evaluation of the four-loop hexagon, which we perform in Section 5. In Section 6 we derive an alternative representation of the configuration-space propagator, and use it to make the four-loop hexagon of Section 4 correspond to a one-loop hexagon

[1] This limit is sufficient for the exact determination of the two-loop hexagon Wilson-loop for arbitrary kinematics.

with massive internal propagators, integrated over the internal masses. We conclude in Section 7 by applying the correspondence we have found for easy boxes to obtain better Feynman parameterizations for non-planar diagrams.

2. A space-time propagator as a one-loop triangle

The basic object entering the evaluation of the vacuum expectation values of a Wilson loop is a scalar propagator in configuration space. For a massless scalar theory in $D = 4 - 2\epsilon_{UV}$ dimensions, this is

$$\Delta(x) \equiv i\int \frac{d^D k}{(2\pi)^D} \frac{e^{-ikx}}{k^2 + i\varepsilon} = \frac{1}{4\pi^{\frac{D}{2}}} \frac{\Gamma\left(\frac{D}{2} - 1\right)}{(-x^2 + i\varepsilon)^{\frac{D}{2}-1}} = \frac{1}{4\pi^{2-\epsilon_{UV}}} \frac{\Gamma(1-\epsilon_{UV})}{(-x^2 + i\varepsilon)^{1-\epsilon_{UV}}}\,. \tag{2.1}$$

There is a correspondence between this propagator and a scalar Feynman diagram. Consider a one-loop triangle with massless internal propagators (Fig. 1)

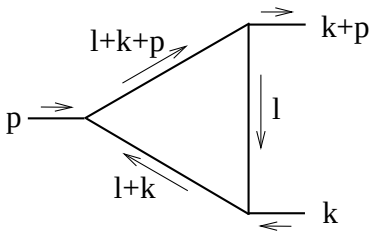

Figure 1: A one-loop triangle with a massless leg p.

$$\mathrm{Tria}(k,p;1,1,1) = \int \frac{d^D\ell}{i\pi^{\frac{D}{2}}} \frac{1}{(\ell^2 + i\varepsilon)\left[(\ell+k)^2 + i\varepsilon\right]\left[(\ell+k+p)^2 + i\varepsilon\right]} \tag{2.2}$$

with

$$p^2 = 0, \quad k^2, (k+p)^2 \neq 0. \tag{2.3}$$

We combine with a Feynman parameter the last two propagators of the above expression,

$$\mathrm{Tria}(k,p;1,1,1) = \int_0^1 d\tau \int \frac{d^D\ell}{i\pi^{\frac{D}{2}}} \frac{1}{\left[\ell^2 + i\varepsilon\right]\left[(\ell+k+\tau p)^2 + i\varepsilon\right]^2}, \tag{2.4}$$

and integrate the loop momentum ℓ in $D = 4 - 2\epsilon$ dimensions. We obtain:

$$\mathrm{Tria}(k,p;1,1,1) = -\Gamma(-\epsilon)\frac{\Gamma(1-\epsilon)\Gamma(1+\epsilon)}{\Gamma(1-2\epsilon)} \int_0^1 \frac{d\tau}{\left[-(k+\tau p)^2 - i\varepsilon\right]^{1+\epsilon}}\,. \tag{2.5}$$

The propagator in the above equation resembles already the configuration space propagator in Eq. (2.1). To make the correspondence explicit we introduce a "space-time point" $x = k$ and a "trajectory" in configuration space $z(\tau) = -\tau p$. By comparing Eq. (2.5) with the propagator in Eq. (2.1), and identifying $\epsilon_{UV} = -\epsilon$, we find

$$\mathrm{Tria}(k,p;1,1,1) = -4\pi^{2+\epsilon}\frac{\Gamma(-\epsilon)\Gamma(1-\epsilon)}{\Gamma(1-2\epsilon)} \int_0^1 d\tau\, \Delta^*(x - z(\tau))\,. \tag{2.6}$$

$\Delta^*(x)$ is the complex conjugate of the propagator $\Delta(x)$ of Eq. (2.1), i.e. is an anti-causal propagator, appearing when evaluating conjugate amplitudes. This correspondence is illustrated in Fig. 2. We notice that the result in Eq. (2.6) is invariant under translations,

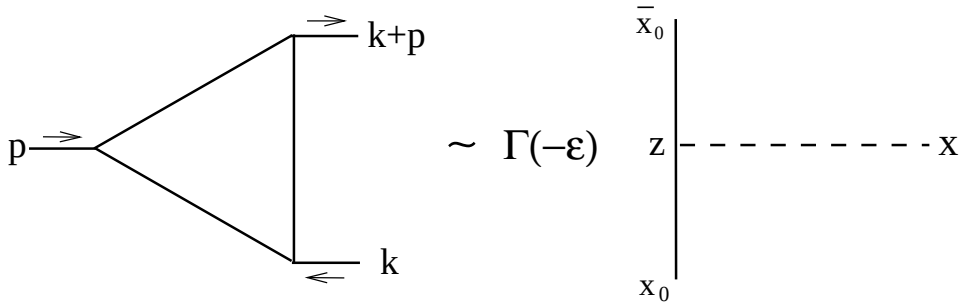

Figure 2: Pictorial representation of the mapping of the triangle into a Wilson line.

so that we can equivalently define $x = x_0 + k$ and $z(\tau) = x_0 - \tau p$, where x_0 is an arbitrary space-time point.

2.1 The triangle rule

We now consider a one-loop triangle (Fig. 3) with general powers of propagators

$$\mathrm{Tria}(k,p;\nu_1,\nu_2,\nu_3) = \int \frac{d^D\ell}{i\pi^{\frac{D}{2}}} \frac{1}{[\ell^2]^{\nu_1}[(\ell+p)^2]^{\nu_2}[(\ell-k)^2]^{\nu_3}}\,. \tag{2.7}$$

We implicitly assume that all denominators are regularized by giving each of them a positive infinitesimal imaginary part. Following the same procedure as above, we derive:

$$\begin{aligned}\mathrm{Tria}(k,p,\nu_1,\nu_2,\nu_3) = (-1)^{\frac{D}{2}} \frac{\Gamma\left(\nu_{123}-\frac{D}{2}\right)}{\Gamma(\nu_1)\Gamma(\nu_2)\Gamma(\nu_3)} \frac{\Gamma\left(\frac{D}{2}-\nu_{12}\right)\Gamma\left(\frac{D}{2}-\nu_3\right)}{\Gamma(D-\nu_{123})} \\ \times \int_0^1 d\tau \frac{(1-\tau)^{\nu_1-1}\tau^{\nu_2-1}}{[(k+\tau p)^2]^{\nu_{123}-\frac{D}{2}}}\,.\end{aligned} \tag{2.8}$$

We notice that, unless $\nu_1 = \nu_2 = 1$, the interpretation of the one-loop triangle as a Wilson-line propagator is lost due to the non-trivial numerator of the integrand. For $\nu_1 = \nu_2 = 1$,

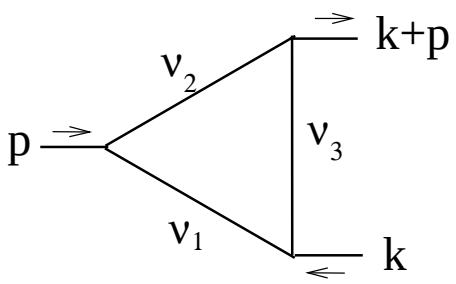

Figure 3: A scalar triangle with arbitrary powers in the propagators.

the one-loop triangle can be interpreted as a propagator attached to a Wilson line, since Eq. (2.8) can be rewritten as follows:

$$\mathrm{Tria}(k,p,1,1,\nu_3) = (-1)^{\nu_3}\frac{\Gamma\left(\nu_3+\epsilon\right)}{\Gamma(\nu_3)}\times \\ \times\frac{\Gamma\left(-\epsilon\right)\Gamma\left(2-\epsilon-\nu_3\right)}{\Gamma(2-2\epsilon-\nu_3)}\int_0^1 d\tau\frac{1}{[-(k+\tau p)^2]^{\nu_3+\epsilon}}\,, \quad (2.9)$$

where we have set $D = 4-2\epsilon$. Comparing with the scalar propagator in Eq. (2.1), we find the correspondence

$$\mathrm{Tria}(k,p,1,1,\nu_3) = (-1)^{\nu_3}\frac{4\pi^{1+\epsilon+\nu_3}\Gamma\left(-\epsilon\right)}{\Gamma(\nu_3)}\frac{\Gamma\left(2-\epsilon-\nu_3\right)}{\Gamma(2-2\epsilon-\nu_3)}\times \\ \times\int_0^1 d\tau\;\Delta^*(x-z(\tau))|_{\epsilon_{UV}=-\epsilon-\nu_3+1}\,, \quad (2.10)$$

where, as before, we have identified k with the space-time point x and have introduced the trajectory $z(\tau) = -\tau p$. Therefore a one-loop triangle $\mathrm{Tria}(k,p,1,1,\nu_3)$ in $D = 4-2\epsilon$ is dual to the propagator in configuration space in $D = 4+2\nu_3+2\epsilon$ dimensions. We remark that the duality of the propagator in configuration space and the one-loop triangle has been also discussed in Refs. [22, 23].[2]

3. The two-loop diagonal box as a one-loop Wilson loop diagram

A question which arises from the duality of the previous section is whether similar dualities exist for more complicated diagrams. We shall show that the two-loop diagonal box diagram in Fig. 4 is dual to a one-loop Wilson-loop diagram. The two-loop diagonal box is

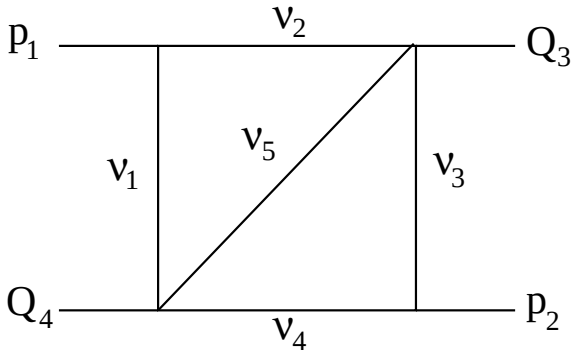

Figure 4: The diagonal box with massless internal propagators raised to arbitrary powers ν_i.

$$\mathrm{DBox}(p_1,p_2,Q_3;\nu_1,\nu_2,\nu_3,\nu_4,\nu_5) = \\ \int\frac{d^Dk\,d^D\ell}{i^2\pi^D}\frac{1}{[k_1^2]^{\nu_1}[(k_1+p_1)^2]^{\nu_2}[k_2^2]^{\nu_3}[(k_2+p_2)^2]^{\nu_4}[\ell^2]^{\nu_5}}\,, \quad (3.1)$$

[2]We thank Gregory Korchemsky for bringing these articles to our attention

where $k_1 = k + \ell$ and $k_2 = k + p_1 + Q_3$. We can cast this integral as

$$\mathrm{DBox}(p_1, p_2, Q_3; \nu_1, \nu_2, \nu_3, \nu_4, \nu_5) = \int \frac{d^D k}{i\pi^{\frac{D}{2}}} \frac{\mathrm{Tria}(k, p, \nu_1, \nu_2, \nu_5)}{[k_2^2]^{\nu_3}[(k_2+p_2)^2]^{\nu_4}} \,. \tag{3.2}$$

and then use the triangle rule of Eq. (2.8) on $\mathrm{Tria}(k, p, \nu_1, \nu_2, \nu_5)$. We obtain

$$\begin{aligned}\mathrm{DBox}(p_1, p_2, Q_3; \nu_1, \nu_2, \nu_3, \nu_4) = (-1)^{\frac{D}{2}} \frac{\Gamma\left(\nu_{125} - \frac{D}{2}\right)}{\Gamma(\nu_1)\Gamma(\nu_2)\Gamma(\nu_5)} \frac{\Gamma\left(\frac{D}{2} - \nu_{12}\right)\Gamma\left(\frac{D}{2} - \nu_5\right)}{\Gamma(D - \nu_{125})} \times \\ \times \int_0^1 d\tau_1 \int \frac{d^D k}{i\pi^{\frac{D}{2}}} \frac{(1-\tau_1)^{\nu_1 - 1} \tau_1^{\nu_2 - 1}}{[(k + \tau_1 p_1)^2]^{\nu_{125} - \frac{D}{2}} [k_2^2]^{\nu_3} [(k_2 + p_2)^2]^{\nu_4}} \,.\end{aligned} \tag{3.3}$$

We recognize that the k integral is another triangle

$$\int \frac{d^D k}{i\pi^{\frac{D}{2}}} \frac{1}{[(k+\tau_1 p_1)^2]^{\nu_{125} - \frac{D}{2}} [k_2^2]^{\nu_3} [(k_2+p_2)^2]^{\nu_4}} = \mathrm{Tria}\left(Q_3 + (1-\tau_1)p_1, p_2, \nu_3, \nu_4, \nu_{125} - \frac{D}{2}\right) , \tag{3.4}$$

and apply again the triangle rule. Our representation of the two-loop diagonal box reads

$$\begin{aligned}\mathrm{DBox}(p_1, p_2, Q_3; \nu_1, \nu_2, \nu_3, \nu_4, \nu_5) = (-1)^D \frac{\Gamma\left(\nu_{12345} - D\right)}{\Gamma(\nu_1)\Gamma(\nu_2)\Gamma(\nu_3)\Gamma(\nu_4)\Gamma(\nu_5)} \times \\ \times \frac{\Gamma\left(\frac{D}{2} - \nu_{12}\right)\Gamma\left(\frac{D}{2} - \nu_{34}\right)\Gamma\left(\frac{D}{2} - \nu_5\right)}{\Gamma\left(\frac{3}{2}D - \nu_{12345}\right)} \times \\ \times \int_0^1 d\tau_1 \int_0^1 d\tau_2 \frac{(1-\tau_1)^{\nu_1 - 1} \tau_1^{\nu_2 - 1} (1-\tau_2)^{\nu_3 - 1} \tau_2^{\nu_4 - 1}}{[((1-\tau_1)p_1 + \tau_2 p_2 + Q_3)^2]^{\nu_{12345} - D}} \,.\end{aligned} \tag{3.5}$$

In the special case $\nu_1 = \nu_2 = \nu_3 = \nu_4 = 1$,

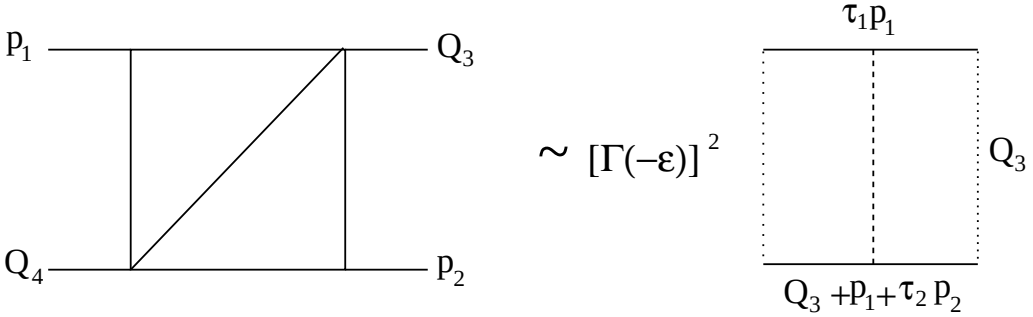

Figure 5: Schematic illustration of the correspondence between the diagonal box and a one-loop scalar Wilson loop.

$$\begin{aligned}\mathrm{DBox}(p_1, p_2, Q_3, 1, 1, 1, 1, \nu_5) = (-1)^{\nu_5} \frac{\Gamma\left(\nu_5 + 2\epsilon\right)\Gamma(2 - \nu_5 - \epsilon)\Gamma^2(-\epsilon)}{\Gamma(2 - \nu_5 - 3\epsilon)\Gamma(\nu_5)} \times \\ \times \int_0^1 d\tau_1 \int_0^1 d\tau_2 \frac{1}{[-(\bar{\tau}_1 p_1 + \tau_2 p_2 + Q_3)^2]^{\nu_5 + 2\epsilon}} \,.\end{aligned} \tag{3.6}$$

We can interpret the two-loop diagonal box as one of the one-loop contributions to the vacuum expectation value of a Wilson loop with an arbitrary number of edges (see Fig. 5). This is accomplished by introducing the trajectories $z(\tau_i) = x_i - \tau_i\, p_i$, ending in the points $\bar{x}_i$ such that $p_i = x_i - \bar{x}_i$. In terms of the x_i and $\bar{x}_i$ the arbitrary momenta Q_3 and Q_4 are given by:

$$Q_3 = \bar{x}_1 - x_2\,, \qquad Q_4 = \bar{x}_2 - x_1\,. \tag{3.7}$$

The exact correspondence is

$$\begin{aligned}\mathrm{DBox}(p_1,p_2,Q_3;1,1,1,1,\nu_5) = (-1)^{\nu_5}\, 4\pi^{1+\nu_5+2\epsilon}\frac{\Gamma(2-\nu_5-\epsilon)\Gamma^2(-\epsilon)}{\Gamma(2-\nu_5-3\epsilon)\Gamma(\nu_5)}\times \\ \times \int_0^1 d\tau_1 \int_0^1 d\tau_2\, \Delta^*(z(\tau_1)-z(\tau_2))|_{\epsilon_{UV}=1-\nu_5-2\epsilon}\,. \end{aligned} \tag{3.8}$$

We further notice that for $Q_3 = 0$ one recovers the cusp contribution to the one-loop Wilson loop.

3.1 The two-loop diagonal box as a one-loop easy box

It is known that the two-loop diagonal box of the previous section and the one-loop easy box are dual.[3] This can be seen easily by comparing their Mellin-Barnes representations [24]. This duality is easy to prove by showing that the one-loop box (in $D = 6-4\epsilon$ dimensions) and the two-loop diagonal box (in $D = 4-2\epsilon$ dimensions) correspond to the same Wilson-loop diagram of the right-hand side of Eq. (3.8).

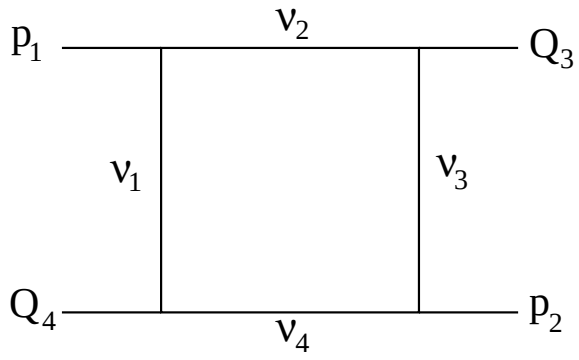

Figure 6: The easy box.

The one-loop "easy box" of Fig. 6 is defined as:

$$\mathrm{Box}(p_1,p_2,Q_3,\nu_1,\nu_2,\nu_3,\nu_4) = \int \frac{d^Dk}{i\pi^{\frac{D}{2}}}\frac{1}{[k_1^2]^{\nu_1}[(k_1+p_1)^2]^{\nu_2}[k_2^2]^{\nu_3}[(k_2+p_2)^2]^{\nu_4}}\,, \tag{3.9}$$

with $k_1 = k$, $k_2 = k+p_1+Q_3$ and $p_1^2 = p_2^2 = 0$. We perform the Feynman parameterization found in Ref. [25]. We first join the two lines separated by p_1 by introducing the Feynman

[3] We thank Bas Tausk for bringing this duality to our attention in private discussions immediately after his publication of Ref. [24], and Lance Dixon for presenting recently to us an independent derivation.

parameter τ_1

$$\begin{aligned}\mathrm{Box}(p_1,p_2,Q_3,\nu_1,\nu_2,\nu_3,\nu_4) &= \frac{\Gamma(\nu_{12})}{\Gamma(\nu_1)\Gamma(\nu_2)}\int_0^1 d\tau_1 \int \frac{d^Dk}{i\pi^{\frac{D}{2}}} \frac{\bar\tau_1^{\nu_1-1}\tau_1^{\nu_2-1}}{[(k_1+\tau_1 p_1)^2]^{\nu_{12}}[k_2^2]^{\nu_3}[(k_2+p_2)^2]^{\nu_4}} \\ &= \frac{\Gamma(\nu_{12})}{\Gamma(\nu_1)\Gamma(\nu_2)}\int_0^1 d\tau_1\, \bar\tau_1^{\nu_1-1}\tau_1^{\nu_2-1}\,\mathrm{Tria}(Q_3+\bar\tau_1 p_1, p_2; \nu_3,\nu_4,\nu_{12})\,. \end{aligned} \tag{3.10}$$

In the above, we used the shorthand notation $\bar\tau_i \equiv 1-\tau_i$, and we recognized that the k integral corresponds to a triangle. Applying the triangle rule Eq. (2.8), we get

$$\begin{aligned}\mathrm{Box}(p_1,p_2,Q_3,\nu_1,\nu_2,\nu_3,\nu_4) &= (-1)^{\frac{D}{2}}\frac{\Gamma\left(\nu_{1234}-\frac{D}{2}\right)}{\Gamma(\nu_1)\Gamma(\nu_2)\Gamma(\nu_3)\Gamma(\nu_4)}\times \\ &\times \frac{\Gamma\left(\frac{D}{2}-\nu_{12}\right)\Gamma\left(\frac{D}{2}-\nu_{34}\right)}{\Gamma\left(D-\nu_{1234}\right)}\int_0^1 d\tau_1\int_0^1 d\tau_2\,\frac{\bar\tau_1^{\nu_1-1}\tau_1^{\nu_2-1}\bar\tau_2^{\nu_3-1}\tau_2^{\nu_4-1}}{[(\bar\tau_1 p_1+\tau_2 p_2+Q_3)^2]^{\nu_{1234}-\frac{D}{2}}}\,. \end{aligned} \tag{3.11}$$

Comparing Eq. (3.11) with Eq. (3.5) we immediately obtain that the diagonal box is proportional to the one-loop easy box in $2(D-\nu_5)$ dimensions. The precise relation is

$$\begin{aligned}\mathrm{Box}_{2(D-\nu_5)}(p_1,p_2,Q_3,\nu_1,\nu_2\nu_3,\nu_4) &= (-1)^{-\nu_5}\frac{\Gamma\left(\frac{3}{2}D-\nu_{12345}\right)}{\Gamma(2D-\nu_{12345}-\nu_5)}\times \\ &\times \frac{\Gamma(D-\nu_{125})}{\Gamma\left(\frac{D}{2}-\nu_{12}\right)}\frac{\Gamma(D-\nu_{345})}{\Gamma\left(\frac{D}{2}-\nu_{34}\right)}\frac{\Gamma(\nu_5)}{\Gamma\left(\frac{D}{2}-\nu_5\right)}\times \\ &\times \mathrm{DBox}_D(p_1,p_2,Q_3,\nu_1,\nu_2,\nu_3,\nu_4,\nu_5)\,. \end{aligned} \tag{3.12}$$

The connection to a Wilson-loop diagram is exact if we specialize Eq. (3.11) to the case $\nu_i = 1$. Replacing $D = 4-2\epsilon$ we obtain

$$\begin{aligned}\mathrm{Box}(p_1,p_2,Q_3,1,1,1,1) &= 2\,\Gamma(-\epsilon)\frac{\Gamma\left(2+\epsilon\right)\Gamma(1-\epsilon)}{\Gamma(1-2\epsilon)}\times \\ &\times \int_0^1 d\tau_1\int_0^1 d\tau_2\,\frac{1}{[-(\bar\tau_1 p_1+\tau_2 p_2+Q_3)^2]^{2+\epsilon}}\,. \end{aligned} \tag{3.13}$$

and, equivalently,

$$\begin{aligned}\mathrm{Box}(p_1,p_2,Q_3,1,1,1,1) &= 8\pi^{3+\epsilon}\,\Gamma(-\epsilon)\frac{\Gamma(1-\epsilon)}{\Gamma(1-2\epsilon)}\times \\ &\times \int_0^1 d\tau_1\int_0^1 d\tau_2\,\Delta^*(z(\tau_1)-z(\tau_2))|_{\epsilon_{UV}=-1-\epsilon}\,, \end{aligned} \tag{3.14}$$

with the trajectories $z(\tau_i)$ being the same as in Fig. 5. Therefore, the one-loop easy box can be interpreted as a one-loop diagram contributing to a Wilson loop with an arbitrary number of edges in $D = 6+2\epsilon$ dimensions. Equivalently, the same Wilson-loop diagram in $D = 4+2\epsilon$ dimensions corresponds to the one-loop easy box diagram in $D = 6-4\epsilon$ dimensions (which is finite).

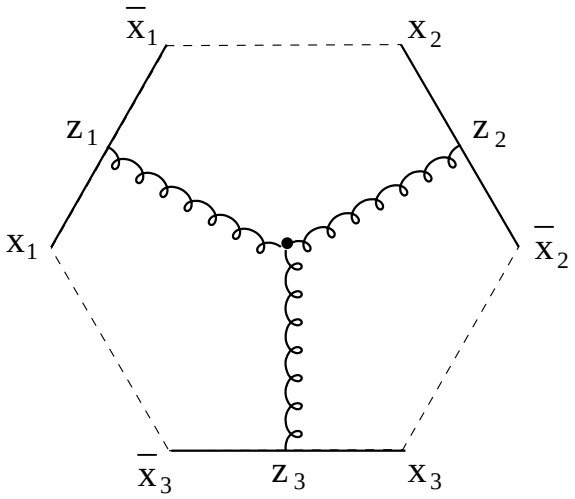

Figure 7: The hard diagram.

4. The hard diagram as a four-loop hexagon

In this section we seek further dualities among Wilson loop diagrams and Feynman diagrams. It has been shown by explicit calculations that the Wilson-loop and loop-amplitude duality holds for two-loop six-leg amplitudes. In the previous section we saw that one-loop Wilson-loop diagrams are mapped naturally to two-loop Feynman diagrams and also, with a handy duality of the two-loop diagonal box and the one-loop "easy box", to one-loop Feynman diagrams.

We now examine the so-called "hard diagram" which contributes to the two-loop Wilson loop. It owes its name to the fact that this has been very difficult to compute analytically for polygon Wilson loops with more than five sides. We shall show that the hard diagram is in fact a four-loop hexagon in disguise. We will first show that the hard diagram can be obtained by acting with a suitable differential operator on a "scalar hard diagram", a special two-loop diagram in configuration space. Then, we will use the triangle rule to map the scalar hard diagram into a four-loop hexagon.

The hard diagram is represented in Fig. 7. There we recognize three trajectories $z(\tau_i)$ for $i = 1, 2, 3$, which depend on the three light-like momenta $\{p_1, p_2, p_3\}$ via the parameterization

$$z(\tau_i) = x_i - \tau_i \, p_i \equiv z_i \, . \tag{4.1}$$

The other three positions $\{\bar{x}_1, \bar{x}_2, \bar{x}_3\}$ are related to three momenta $\{Q_1, Q_2, Q_3\}$, which can be off-shell or on-shell, as follows:

$$\bar{x}_1 - x_2 = Q_3 \, , \quad \bar{x}_2 - x_3 = Q_1 \, , \quad \bar{x}_3 - x_1 = Q_2 \, . \tag{4.2}$$

The above distances represent the insertion of an arbitrary number of sides which are not connected with gluon propagators. The minimum number of sides for which all Q_i are non-zero is six, in which case $\{Q_1, Q_2, Q_3\}$ are light-like.

Neglecting colour and symmetry factors, the explicit expression for the hard diagram reads

$$\begin{aligned}\mathrm{Hard}(p_1,p_2,p_3,Q_1,Q_2,Q_3) &= p_1^{\mu_1}p_2^{\mu_2}p_3^{\mu_3}\int_0^1\left(\prod_{i=1}^3 d\tau_i\right)\\ &\times V^{\mu_1\mu_2\mu_3}\int\frac{i\,d^dz}{\pi^{d/2}}\,\Delta\left(z-z(\tau_1)\right)\,\Delta\left(z-z(\tau_2)\right)\,\Delta\left(z-z(\tau_3)\right)\,. \end{aligned}\tag{4.3}$$

Here we have indicated with $d=4-2\epsilon_{UV}$, the dimension of the configuration space in which the hard diagram lives, and $V^{\mu_1\mu_2\mu_3}$ is a differential operator that represents the three-gluon vertex:

$$V^{\mu_1\mu_2\mu_3}=\eta^{\mu_1\mu_2}(\partial_1^{\mu_3}-\partial_2^{\mu_3})+\eta^{\mu_2\mu_3}(\partial_2^{\mu_1}-\partial_3^{\mu_1})+\eta^{\mu_1\mu_3}(\partial_3^{\mu_2}-\partial_1^{\mu_2})\,,\tag{4.4}$$

where we have used the notation $\partial_i^\mu\equiv\partial/\partial z_i^\mu$. Exploiting now the relations

$$\begin{aligned} x_1-x_2&=p_1+Q_3 \qquad & z_1-z_2&=\bar\tau_1p_1+\tau_2p_2+Q_3\,,\\ x_2-x_3&=p_2+Q_1 \qquad & z_2-z_3&=\bar\tau_2p_2+\tau_3p_3+Q_1\,,\\ x_3-x_1&=p_3+Q_2 \qquad & z_3-z_1&=\bar\tau_3p_3+\tau_1p_1+Q_2\,, \end{aligned}\tag{4.5}$$

we can rewrite the tree-gluon vertex in terms of derivatives with respect to the external momenta $\{Q_1,Q_2,Q_3\}$ only. Introducing the new differential operator

$$\begin{aligned}\tilde V_{\mu_1\mu_2\mu_3} &= \eta_{\mu_1\mu_2}\left(2\frac{\partial}{\partial Q_3^{\mu_3}}-\frac{\partial}{\partial Q_1^{\mu_3}}-\frac{\partial}{\partial Q_2^{\mu_3}}\right)\\ &+\eta_{\mu_2\mu_3}\left(2\frac{\partial}{\partial Q_1^{\mu_1}}-\frac{\partial}{\partial Q_2^{\mu_1}}-\frac{\partial}{\partial Q_3^{\mu_1}}\right)\\ &+\eta_{\mu_1\mu_3}\left(2\frac{\partial}{\partial Q_2^{\mu_2}}-\frac{\partial}{\partial Q_1^{\mu_2}}-\frac{\partial}{\partial Q_3^{\mu_2}}\right)\,,\end{aligned}\tag{4.6}$$

and exploiting the fact that the integral in Eq. (4.3) is finite, we can extract $\tilde V_{\mu_1\mu_2\mu_3}$ from the z integral and write

$$\mathrm{Hard}(p_1,p_2,p_3,Q_1,Q_2,Q_3)=p_1^{\mu_1}p_2^{\mu_2}p_3^{\mu_3}\,\tilde V_{\mu_1\mu_2\mu_3}\mathrm{SHard}(p_1,p_2,p_3,Q_1,Q_2,Q_3)\,.\tag{4.7}$$

Here we have introduced a "scalar hard diagram", defined by:

$$\mathrm{SHard}(p_1,p_2,p_3,Q_1,Q_2,Q_3)=\int_0^1\left(\prod_{i=1}^3 d\tau_i\right)\int\frac{i\,d^dz}{\pi^{d/2}}\,\prod_{i=1}^3\Delta\left(z-z(\tau_i)\right)\,.\tag{4.8}$$

We can turn the scalar hard diagram into a Feynman diagram in momentum space. First, we introduce three momenta $k_i=z-x_i$ and identify the position z we are integrating over with the loop momentum $k=z-x_1=k_1$. Substituting the representation in Eq. (2.6) for each propagator $\Delta(z-z_i)$ we obtain

$$\begin{aligned}\mathrm{SHard}(p_1,p_2,p_3,Q_1,Q_2,Q_3) &= \left(-\frac{\Gamma(1-2\epsilon)}{4\pi^{2+\epsilon}\Gamma(-\epsilon)\Gamma(1-\epsilon)}\right)^3\times\\ &\times\int\frac{i\,d^dk}{\pi^{d/2}}\,\prod_{i=1}^3\left[\mathrm{Tria}(k_i,p_i,1,1,1)\right]^*\,,\end{aligned}\tag{4.9}$$

where, as in the previous section, we have taken the complex conjugate of the triangle to account for the fact that the $i\varepsilon$ prescription of the scalar propagators in $\mathrm{Tria}(k_i, p_i; 1, 1, 1)$ is reversed with respect to the propagators in configuration space in Eq. (4.8). We further replace each triangle $\mathrm{Tria}(k_i, p_i, 1, 1, 1)$ with its explicit expression of Eq. (2.2), and rewrite the scalar hard diagram as

$$\mathrm{SHard}(p_1, p_2, p_3, Q_1, Q_2, Q_3) = \left(-\frac{\Gamma(1-2\epsilon)}{4\pi^{2+\epsilon}\Gamma(-\epsilon)\Gamma(1-\epsilon)}\right)^3 \times \\ \times \int \frac{i\, d^d k}{\pi^{d/2}} \left(\prod_{i=1}^{3} \frac{d^D \ell_i}{i\pi^{\frac{D}{2}}} \frac{1}{\ell_i^2\,(\ell_i + k_i)^2\,(\ell_i + k_i + p_i)^2}\right) . \quad (4.10)$$

Notice that the dimension of the ℓ integral is $D = 4 - 2\epsilon$, as in Eq. (2.2). The k integration is, however, in $d = 4 - 2\epsilon_{UV} = 4 + 2\epsilon$ dimensions. We remark that the diagram is finite for $\epsilon = -\epsilon_{UV} = 0$, and insensitive to the regularization prescription of the various integrations. We observe now that, using the definitions of the momenta $k_i = z - x_i$ in terms of the positions x_i, and the relations between the "distances" $x_{i+1} - x_i$ in Eq. (4.5), we can express k_i in terms of the light-like momenta $\{p_1, p_2, p_3\}$ and of three further momenta $\{Q_1, Q_2, Q_3\}$ as follows

$$k_1 = k\,, \quad k_2 = k + p_1 + Q_3\,, \quad k_3 = k - p_3 - Q_2\,. \quad (4.11)$$

We then recognize that the integral in Eq. (4.10) resembles the four-loop hexagon shown in Fig. 8:

$$\mathrm{Hexa}^{(4)}(p_1, p_2, p_3, Q_1, Q_2, Q_3) = \int \frac{d^D k}{i\pi^{\frac{D}{2}}} \left(\prod_{i=1}^{3} \frac{d^D \ell_i}{i\pi^{\frac{D}{2}}} \frac{1}{\ell_i^2\,(\ell_i + k_i)^2\,(\ell_i + k_i + p_i)^2}\right) . \quad (4.12)$$

We notice that the correspondence is exact only in strictly $D = 4$ dimensions because the

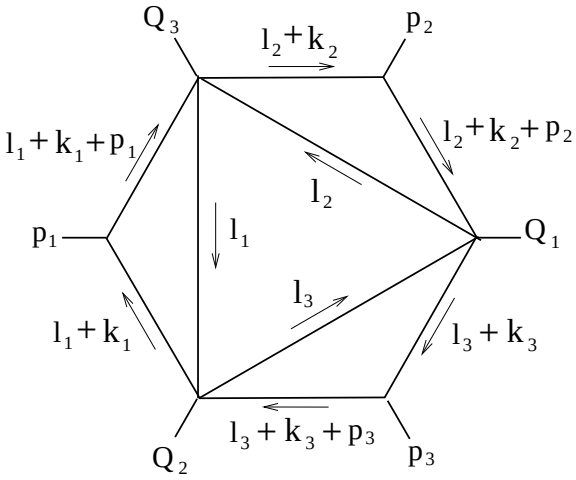

Figure 8: A four-loop scalar hexagon.

k integrals in Eq. (4.10) and Eq. (4.12) have to be performed in two different dimensions. This correspondence, represented in Fig. 9, gives promise to derive the finite value of the hard diagram from the leading $1/\epsilon^3$ pole of the four-loop hexagon,

$$\text{SHard}(p_1,p_2,p_3,Q_1,Q_2,Q_3)|_{d=4} = \left(\frac{1}{4\pi^2}\right)^3 \times \\ \times \lim_{\epsilon\to 0} \epsilon^3 \, [\text{Hexa}^{(4)}(p_1,p_2,p_3,Q_1,Q_2,Q_3)]^* \Big|_{D=4-2\epsilon} \,, \quad (4.13)$$

using factorization properties of collinear singularities. The determination of this coefficient

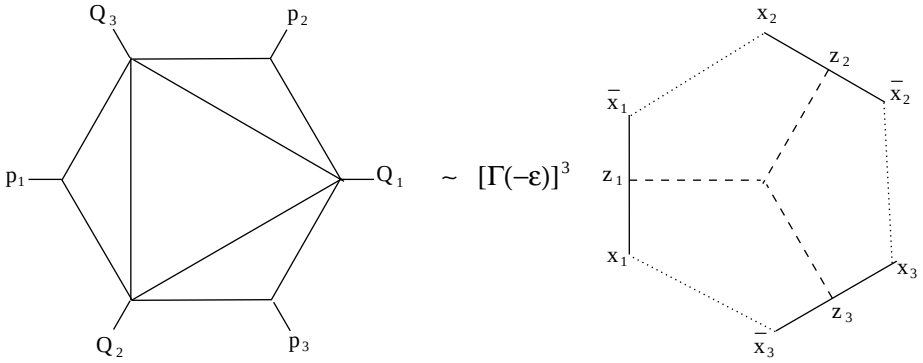

Figure 9: Pictorial representation of the correspondence between a four-loop hexagon and a diagram in configure space.

would give the analytic answer for the two-loop vacuum expectation value of a polygon Wilson loop with an arbitrary number of sides. We leave this calculation for future work.

5. Numerical evaluation of a four-loop hexagon Feynman diagram

The dualities that we are exploring in this paper could facilitate Feynman diagram calculations. We have not yet explored their full potential. However, benefits in computing numerically the multi-loop Feynman diagrams which enter these dualities are striking. From the Wilson-loop side of the correspondence, the hard diagram is only difficult to compute analytically and it can be evaluated numerically rather easily. As we have seen in the previous section, this diagram is dual to a very complicated four-loop hexagon. We can use the duality to compute such a complicated Feynman integral. To the best of our knowledge, there has been no four-loop Feynman integral with six legs evaluated in the literature.

We start from the explicit expression for the hexagon in Eq. (4.12) and replace each triangle subgraph with its representation in terms of a scalar propagator $\Delta(x)$ in Eq. (2.6). Using the correspondence between momenta and space-time points introduced in Eq. (4.5),

we obtain the following representation:

$$\text{Hexa}^{(4)}(p_1,p_2,p_3,Q_1,Q_2,Q_3) = \left(-4\pi^{2+\epsilon}\frac{\Gamma(-\epsilon)\,\Gamma(1-\epsilon)}{\Gamma(1-2\epsilon)}\right)^3 \times \\ \times \int_0^1 \prod_{i=1}^3 d\tau_i \int \frac{d^D z}{i\pi^{\frac{D}{2}}}\,\Delta^*(z)\,\Delta^*(z+z_{12})\,\Delta^*(z-z_{31})\,, \quad (5.1)$$

where the scalar propagators $\Delta(x)$ are in $4+2\epsilon$ dimensions, while the z integral has to be performed in $4-2\epsilon$ dimensions. We now substitute the explicit expression for $\Delta(x)$, introduce a further Feynman parameterization of the z integral so as to write the product of propagators as a single denominator, and finally perform the z integration to get:

$$\text{Hexa}^{(4)}(p_1,p_2,p_3,Q_1,Q_2,Q_3) = \left(\frac{\Gamma(-\epsilon)\,\Gamma(1-\epsilon)}{\Gamma(1-2\epsilon)}\right)^3 \Gamma(1+4\epsilon)\times \\ \times \int_0^1 \left(\prod_{i=1}^3 d\tau_i\right) \int_0^1 \left(\prod_{i=1}^3 d\alpha_i\right) \delta\left(1-\sum_{i=1}^3 \alpha_i\right) \frac{(\alpha_1\alpha_2\alpha_3)^\epsilon}{[-(\alpha_1\alpha_2 z_{12}^2+\alpha_2\alpha_3 z_{23}^2+\alpha_3\alpha_1 z_{31}^3+i\varepsilon)]^{1+4\epsilon}}\,. \quad (5.2)$$

We obtain an expression for the four-loop hexagon that is a function of only five Feynman parameters, and that depends on the coordinates z_i only through the distances $z_{i,i+1}$ introduced in Eq. (4.5). This representation offers the further advantage that all collinear singularities of the hexagon graph have been captured as a divergent $1/\epsilon^3$ prefactor. The integral is finite in all limits and can be expanded directly around $\epsilon = 0$.

This scalar integral depends on twelve invariants:

$$\{s_1,\ldots,s_{12}\} = \{(p_1p_2),(p_1p_3),(p_2p_3),(p_1Q_3),(p_3Q_1),(p_3Q_2), \\ (p_2Q_3),(p_1Q_2),(p_2Q_1),Q_1^2,Q_2^2,Q_3^2\}\,. \quad (5.3)$$

For illustration of numerical results we consider the case in which all momenta, Q_i,p_i are light-like, so that the final result depends only on $\{s_1,\ldots,s_9\}$. We cast the result in the form:

$$\text{Hexa}^{(4)}(p_1,p_2,p_3,Q_1,Q_2,Q_3) = \Gamma(1+4\epsilon)\left(\frac{A_{-3}}{\epsilon^3}+\frac{A_{-2}}{\epsilon^2}+\frac{A_{-1}}{\epsilon}+A_0\right)\,. \quad (5.4)$$

The results of the numerical integration for two specific sets of invariants are displayed in table 1.

$\{s_1,\ldots,s_9\}$	A_{-3}	A_{-2}	A_{-1}	A_0
$\{-1,-1,-1,-1,-1,-1,-1,-1,-1\}$	$-1.04683(4)$	$1.2968(1)$	$1.7337(2)$	$1.9918(4)$
$\{-0.1,-0.2,-0.3,-0.2,-0.4,-0.6,-1,-0.15,-0.25\}$	$-2.80209(2)$	$-7.7878(7)$	$-4.993(2)$	$18.496(6)$

Table 1: Numerical evaluation of the four-loop hexagon for different values of the kinematical invariants.

It is intriguing that this four-loop hexagon can be mapped to a one-loop triangle with non-integers powers of propagators. From the above Feynman parameterization we read that

$$\begin{aligned}\mathrm{Hexa}^{(4)}(p_1,p_2,p_3,Q_1,Q_2,Q_3) = \left(\frac{\Gamma(-\epsilon)\Gamma(1-\epsilon)}{\Gamma(1+\epsilon)\Gamma(1-2\epsilon)}\right)^3 \int_0^1 d\tau_1 d\tau_2 d\tau_3 \\ \times \mathrm{Tria}(\bar\tau_1 p_1 + \tau_2 p_2 + Q_3, \bar\tau_2 p_2 + \tau_3 p_3 + Q_1, 1+\epsilon, 1+\epsilon, 1+\epsilon)\,. \end{aligned} \tag{5.5}$$

Equivalently, the scalar Wilson-loop "hard diagram" through order $\mathcal{O}(\epsilon^0)$ is also proportional to the same integral over the one-loop triangle in the right-hand side of the above equation (with a non-divergent prefactor) [17],

$$\begin{aligned}\mathrm{SHard}(p_1,p_2,p_3,Q_1,Q_2,Q_3) = \frac{1}{(4\pi)^3} \int_0^1 d\tau_1 d\tau_2 d\tau_3 \\ \times \mathrm{Tria}(\bar\tau_1 p_1 + \tau_2 p_2 + Q_3, \bar\tau_2 p_2 + \tau_3 p_3 + Q_1, 1, 1, 1) + \mathcal{O}(\epsilon). \end{aligned} \tag{5.6}$$

In this paper and in Ref. [17] equations like the above (5.5-5.6) have been used for numerical evaluations of the integrals on their left-hand side. However, we believe that they are likely to be a good starting point for an analytic evaluation. We remark that the Tria function is expressed rather compactly in terms of Appell F_4 functions for arbitrary powers of propagators [26, 27, 28].

6. The "hard" Wilson-loop diagram as a massive one-loop hexagon

Wilson-loop integrals can be cast as massive loop Feynman integrals, integrated over their mass parameters. For an arbitrary momentum q

$$\int_0^\infty dm^2 \frac{(m^2)^{-\epsilon}}{[(q^2-m^2+i\varepsilon)^2]^n} = (-1)^n \frac{\Gamma(1-\epsilon)\Gamma(n-1+\epsilon)-1}{\Gamma(n)} [-q^2-i\varepsilon]^{n-1+\epsilon}. \tag{6.1}$$

For $n=2$, we obtain a representation of the propagator in configuration space:

$$\Delta^*(q) = \frac{1}{4\pi^{2+\epsilon}} \frac{\Gamma(1+\epsilon)}{(-q^2-i\varepsilon)^{1+\epsilon}} = \frac{1}{4\pi^{2+\epsilon}\Gamma(1-\epsilon)} \int_0^\infty dm^2 \frac{(m^2)^{-\epsilon}}{[q^2-m^2+i\varepsilon]^2}. \tag{6.2}$$

For a propagator connecting a fixed point $x_0 = -k$ and a light-like line segment $x(\tau) = \tau p$, we have $q = k + \tau p$. Performing the τ integral we have

$$\int_0^1 d\tau \Delta^*(k+\tau p) = \frac{1}{4\pi^{2+\epsilon}\Gamma(1-\epsilon)} \int_0^\infty dm^2 \frac{(m^2)^{-\epsilon}}{[k^2-m^2+i\varepsilon]\,[(k+p)^2-m^2+i\varepsilon]}\,. \tag{6.3}$$

The same relation (up to prefactors) holds for the dual one-loop triangle. We find

$$\mathrm{Tria}(k,p;1,1,1) = \frac{\Gamma(-\epsilon)}{\Gamma(1-2\epsilon)} \int_0^\infty dm^2 \frac{(m^2)^{-\epsilon}}{(k^2-m^2+i\varepsilon)\,[(k+\tau p)^2-m^2+i\varepsilon]}\,. \tag{6.4}$$

This correspondence, pictorially represented in Fig. 10, leads to a different representation

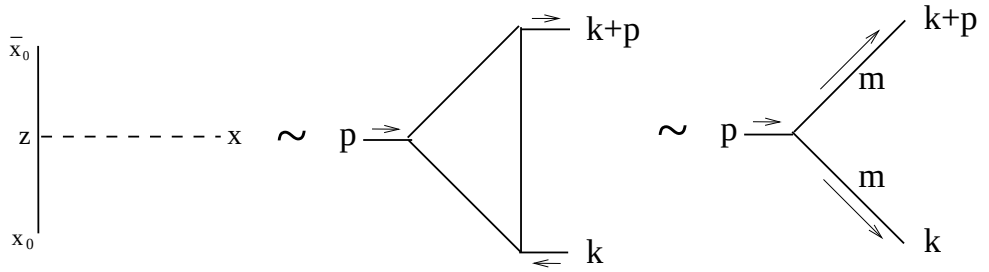

Figure 10: Pictorial representation of the one-loop triangle as an integral over masses.

for the four-loop hexagon considered in Section 4 and displayed in Fig. 8 and, equivalently, for the "hard" Wilson-loop diagram. We find:

$$\mathrm{Hexa}^{(4)}(p_1,p_2,p_3,Q_1,Q_2,Q_3) = \left(\frac{\Gamma(-\epsilon)}{\Gamma(1-2\epsilon)}\right)^3 \times \\ \times \int \frac{d^4k}{i\pi^2} \int_0^\infty \prod_{i=1}^3 dm_i^2 \frac{(m_i^2)^{-\epsilon}}{(k_i^2 - m_i^2 + i\varepsilon)[(k_i+p_i)^2 - m_i^2 + i\varepsilon]}\,, \quad (6.5)$$

where $k_1 = k$, $k_2 = k + p_1 + Q_3$ and $k_3 = k - Q_2 - p_3$. Similarly, the Wilson-loop hard diagram can be written as (see Fig. 11)

$$\mathrm{SHard}^*(p_1,p_2,p_3,Q_1,Q_2,Q_3) = \left(-4\pi^{2+\epsilon}\Gamma(1-\epsilon)\right)^3 \times \\ \times \int \frac{d^4k}{i\pi^2} \int_0^\infty \prod_{i=1}^3 dm_i^2 \frac{(m_i^2)^{-\epsilon}}{(k_i^2 - m_i^2 + i\varepsilon)[(k_i+p_i)^2 - m_i^2 + i\varepsilon]}\,. \quad (6.6)$$

The four-dimensional massive one-loop hexagon can be evaluated analytically after reduc-

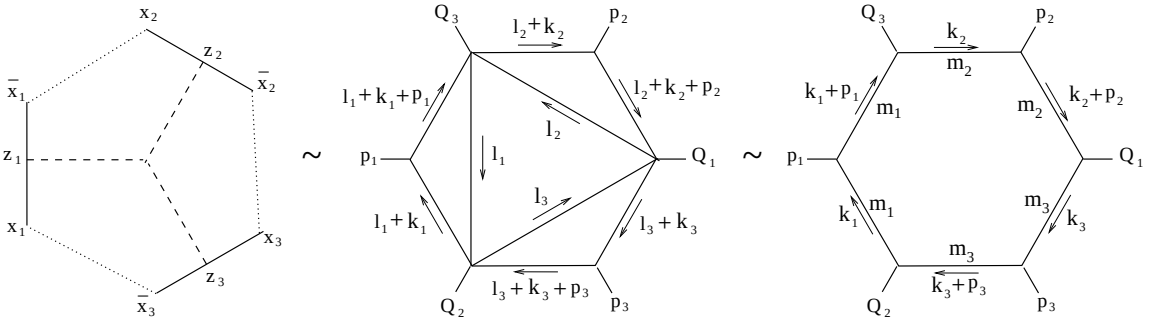

Figure 11: Representation of the mapping of a four-loop hexagon into a one-loop hexagon integrated over internal masses.

ing to box master integrals. The analytic integration over the masses m_i is a formidable task. However, it holds promise for achieving an analytic evaluation of the hard diagram for a Wilson loop with an arbitrary number of sides.

7. Non-planar Feynman integrals

An intriguing feature of Eq. (3.11) is that an "easy box" is cast as a single scalar propagator raised to a dimension-dependent power. Such boxes can be subgraphs of more complicated higher loop non-planar diagrams. Eq. (3.11) can be then utilized to cast these non-planar diagrams as planar diagrams with one loop less, integrated over a range of linear combinations for their external momenta.

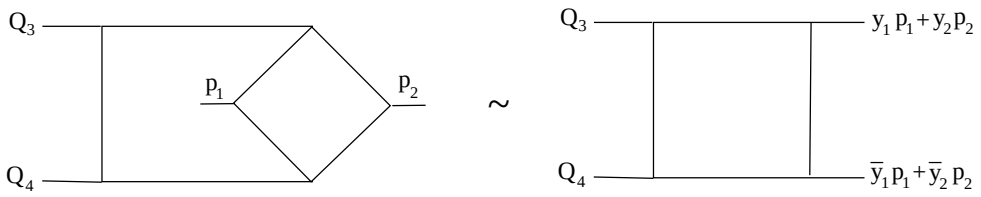

Figure 12: Cross box diagrams contributing to $2 \to 2$ processes.

The two-loop non-planar box integral XBox at the left of Fig. 12 has a one-loop "easy-box" subgraph. Applying Eq. (3.11), we obtain a representation as an integral

$$\begin{aligned}\text{XBox} = 2\,(-1)^{-\epsilon}\,\Gamma(2+\epsilon)\,\frac{\Gamma(-\epsilon)\Gamma(1-\epsilon)}{\Gamma(1-2\epsilon)}\int_0^1 dy_1 \int_0^1 dy_2 \times \\ \times\,\mathcal{F}\left((p_1+p_2)^2,(y_1p_1+y_2p_2+Q_3)^2,(y_1p_1+y_2p_2)^2,(\bar{y}_1p_1+\bar{y}_2p_2+Q_3)^2,Q_3^2\right), \quad (7.1)\end{aligned}$$

over a box function

$$\begin{aligned}\mathcal{F}\left((p_1+p_2)^2,(y_1p_1+y_2p_2+Q_3)^2,(y_1p_1+y_2p_2)^2,(\bar{y}_1p_1+\bar{y}_2p_2+Q_3)^2,Q_3^2\right) = \\ \int \frac{d^Dk}{i\pi^{\frac{D}{2}}}\frac{1}{k^2\left[(k+y_1p_1+y_2p_2)^2\right]^{2+\epsilon}(k+p_1+p_2)^2(k+p_1+p_2+Q_3)^2}, \quad (7.2)\end{aligned}$$

with one of the propagators raised to a non-integer power.

We observe that this representation requires at most five Feynman parameters (three for the box-function in the integrand and y_1, y_2). A naive Feynman representation would yield a six-dimensional integral. One-loop box integrals have been studied extensively in the literature. In Eq. (7.1) it is required a box integral with a non-integer power for one of the propagators. For $Q_3^2 = Q_4^2$ this is known to be a sum of four F_4 hypergeometric functions [28, 29] with well studied analytic continuation properties and asymptotic limits in the mathematical literature.

For a direct numerical evaluation with the method of sector decomposition [30] this Feynman representation is better suited requiring less than half the number of sectors of a naive parameterization. Applying the non-linear transformations of Ref. [31] to factorize infrared singularities is also a much simpler task with our parameterization. Non-planar box diagrams with light-like external legs pose an additional difficulty for their evaluation due to not having a Euclidean region when the Mandelstam variables $s = (p_1+p_2)^2$, $t = (p_2+Q_3)^2$, $u = (Q_3+p_1)^2$ are consistent with momentum conservation:

$$Q_3^2 = Q_4^2 = s+t+u = 0. \quad (7.3)$$

The on-shell limit of an external leg does not commute with the $\epsilon = 0$ of the dimensional regulator due to the emergence of new collinear divergences. It is easy to obtain a Feynman representation with a Euclidean region for generic s, t, u from Eq. (7.1) which possesses the same infrared singularities as for $s, t, u = -s - t$. This is,

$$\text{XBox} = 2\,(-1)^{-\epsilon}\,\Gamma(2+\epsilon)\,\frac{\Gamma(-\epsilon)\Gamma(1-\epsilon)}{\Gamma(1-2\epsilon)}\,\int_0^1 dy_1 \int_0^1 dy_2 \times \\ \times\,\mathcal{F}\left(s, y_1\bar{y}_2 t + y_2\bar{y}_1 u, y_1 y_2 s, \bar{y}_1\bar{y}_2 s, 0\right), \quad (7.4)$$

where we have used momentum conservation only for the second argument of the $\mathcal{F}$ box function.

Using the Mellin-Barnes representation of the one-loop box with two off-shell legs, and introducing one additional Mellin-Barnes integration, we can integrate out all Feynman parameters. We obtain

$$\text{XBox}(p_1, p_2, Q_3; 0, 0, 0) = -2\,\frac{\Gamma(-\epsilon)\Gamma(1-\epsilon)}{\Gamma(-1-3\epsilon)\Gamma(1-2\epsilon)}\int_{-i\infty}^{i\infty}\left(\prod_{i=1}^{4}\frac{d\xi_i}{2\pi i}\Gamma(-\xi_i)\right)\times \\ \times\,\Gamma(3+2\epsilon+\xi_{1234})\Gamma(2+\epsilon+\xi_{1234})\Gamma(-2-2\epsilon-\xi_{134})\Gamma(-2-2\epsilon-\xi_{234})\times \\ \times\,\frac{\Gamma(1+\xi_{34})\Gamma(1+\xi_{13})\Gamma(1+\xi_{14})\Gamma(1+\xi_{23})\Gamma(1+\xi_{24})}{\Gamma^2(2+\xi_{1234})}(-s)^{-3-2\epsilon-\xi_{34}}(-t)^{\xi_3}(-u)^{\xi_4}, \quad (7.5)$$

which is the representation obtain in ref. [24].

Similarly simplified Feynman parameterizations of non-planar diagrams with "easy-box" insertions can be also obtained for integrals with higher number of loops or legs.

8. Conclusions

We have observed dualities among diagrams which enter the calculation of the vacuum expectation value of Wilson loops and scalar Feynman integrals. These can be pictured as:

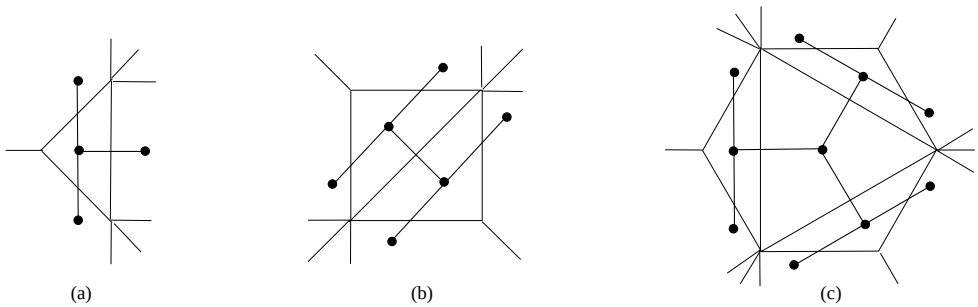

where the meaning of each diagram is:

(a) a one-loop triangle is dual to a scalar propagator in configuration space attached to a Wilson line;

(b) a two-loop diagonal box (and a one-loop easy box) are dual to a scalar propagator connecting two Wilson lines, in fact a one-loop Wilson-loop with an arbitrary number of edges;

(c) a four-loop hexagon is dual to a three-boson vertex connected via scalar propagators to three Wilson lines, which is the so-called two-loop "hard diagram".

A remarkable feature of the representations we have obtained is that the Wilson-line diagram appears always as a factor multiplying a singularity of the corresponding scalar multi-loop diagram. This factorization property has two main advantages. On one hand, if one wishes to exploit a duality to compute an unknown Wilson-loop diagram, it is in general enough to extract the coefficient of the leading singularity of the corresponding scalar integral, which is far easier than fully computing the integral itself. On the other hand, given a scalar multi-loop integral, the corresponding Wilson-loop diagram provides automatically a nice Feynman parameterization for it. In particular, given the fact that part of the singularities are already extracted and that Wilson loops are generally simple to compute numerically, one can use the duality to tackle calculations that would appear impossible at first sight. For illustration of the potential our observations, we compute for the first time in the literature a four-loop hexagon integral, which is dual to the Wilson-loop "hard diagram".

The relations we have found concern planar diagrams only. However, they can be also used when a planar diagram is part of a larger non-planar diagram. For instance, one can use the duality between the one-loop easy box and a scalar propagator to derive a simple Feynman parameterization for the two-loop cross-box, yielding a better starting point for its numerical evaluation [31]. The very same parameterization simplifies the calculation of the cross-box using Mellin-Barnes techniques.

To conclude, the dualities we have found look very promising, and can lead to significant simplifications in the calculation of high-loop integrals appearing both in QCD and in other theories like $\mathcal{N} = 4$ Super Yang-Mills or $\mathcal{N} = 8$ Supergravity. We are looking forward to further investigations on these dualities in the future.

Acknowledgments. We thank Andreas Brandhuber, Lance Dixon, Vittorio del Duca, Claude Duhr, Thomas Gehrmann, Gregory Korchemsky, Eric Laenen, Lorenzo Magnea, Volodya Smirnov, Bas Tausk and Gang Yang for useful discussions. We thank especially Bas Tausk for communicating his insight on the diagonal-box/one-loop box duality in the past. This work is supported by the ERC Starting Grant project IterQCD.

References

[1] J. M. Maldacena, *The large N limit of superconformal field theories and supergravity*, Adv. Theor. Math. Phys. **2** (1998) 231 [Int. J. Theor. Phys. **38** (1999) 1113] [hep-th/9711200].

[2] J. A. Minahan and K. Zarembo, *The Bethe-ansatz for N = 4 super Yang-Mills*, JHEP **0303** (2003) 013 [hepth0212208].

[3] N. Beisert, S. Frolov, M. Staudacher and A. A. Tseytlin, Precision spectroscopy of AdS/CFT,' JHEP **0310** (2003) 037 [hep-th/0308117], and references therein.

[4] N. Beisert and M. Staudacher, *Long-range $PSU(2,2|4)$ Bethe ansaetze for gauge theory and strings*, Nucl. Phys. B **727** (2005) 1 [hep-th/0504190], and references therein.

[5] C. Anastasiou, Z. Bern, L. J. Dixon and D. A. Kosower, *Planar amplitudes in maximally supersymmetric Yang-Mills theory*, Phys. Rev. Lett. **91** (2003) 251602 [hep-th/0309040].

[6] Z. Bern, L. J. Dixon and V. A. Smirnov, *Iteration of planar amplitudes in maximally supersymmetric Yang-Mills theory at three loops and beyond*, Phys. Rev. D **72** (2005) 085001, [hep-th/0505205].

[7] F. Cachazo, M. Spradlin and A. Volovich, *Iterative structure within the five-particle two-loop amplitude*, Phys. Rev. D **74** (2006) 045020 [hep-th/0602228].

[8] Z. Bern, M. Czakon, D. A. Kosower, R. Roiban and V. A. Smirnov, *Two-loop iteration of five-point $N = 4$ super-Yang-Mills amplitudes*, Phys. Rev. Lett. **97** (2006) 181601 [hep-th/0604074].

[9] Z. Bern, L. J. Dixon, D. A. Kosower, R. Roiban, M. Spradlin, C. Vergu and A. Volovich, *The Two-Loop Six-Gluon MHV Amplitude in Maximally Supersymmetric Yang-Mills Theory*, Phys. Rev. D **78** (2008) 045007 [0803.1465[hep-th]].

[10] L. F. Alday and J. Maldacena, *Gluon scattering amplitudes at strong coupling*, JHEP **0706** (2007) 064 [0705.0303[hep-th]].

[11] G. P. Korchemsky, J. M. Drummond and E. Sokatchev, *Conformal properties of four-gluon planar amplitudes and Wilson loops*, Nucl. Phys. B **795** (2008) 385 [0707.0243[hep-th]].

[12] A. Brandhuber, P. Heslop and G. Travaglini, *MHV Amplitudes in N=4 Super Yang-Mills and Wilson Loops*, Nucl. Phys. B **794** (2008) 231 [0707.1153[hep-th]].

[13] J. M. Drummond, J. Henn, G. P. Korchemsky and E. Sokatchev, *Hexagon Wilson loop = six-gluon MHV amplitude*, Nucl. Phys. B **815** (2009) 142 [0803.1466[hep-th]].

[14] A. Brandhuber, P. Heslop, P. Katsaroumpas, D. Nguyen, B. Spence, M. Spradlin and G. Travaglini, *A Surprise in the Amplitude/Wilson Loop Duality*, JHEP **1007** (2010) 080 [1004.2855[hep-th]].

[15] V. Del Duca, C. Duhr and V. A. Smirnov, *An Analytic Result for the Two-Loop Hexagon Wilson Loop in $N = 4$ SYM*, JHEP **1003** (2010) 099 [0911.5332[hep-ph]].

[16] V. Del Duca, C. Duhr and V. A. Smirnov, *The Two-Loop Hexagon Wilson Loop in $N = 4$ SYM* JHEP **1005** (2010) 084 [1003.1702[hep-th]].

[17] C. Anastasiou, A. Brandhuber, P. Heslop, V. V. Khoze, B. Spence and G. Travaglini, *Two-Loop Polygon Wilson Loops in N=4 SYM,* JHEP **0905** (2009) 115 [0902.2245[hep-th]].

[18] M. B. Green, J. H. Schwarz and L. Brink, *N=4 Yang-Mills And N=8 Supergravity As Limits Of String Theories*, Nucl. Phys. B **198** (1982) 474.

[19] Z. Bern, J. S. Rozowsky and B. Yan, *Two-loop four-gluon amplitudes in $\mathcal{N} = 4$ super-Yang-Mills*, Phys. Lett. B **401** (1997) 273 [hep-ph/9702424].

[20] J. M. Drummond, J. Henn, G. P. Korchemsky and E. Sokatchev, *Conformal Ward identities for Wilson loops and a test of the duality with gluon amplitudes*, Nucl. Phys. B **826** (2010) 337 [0712.1223[hep-th]].

[21] V. Del Duca, C. Duhr and V. A. Smirnov, *A Two-Loop Octagon Wilson Loop in $N = 4$ SYM*, JHEP **1009** (2010) 015 [1006.4127[hep-th]].

[22] A. Gorsky and A. Zhiboedov, *One-loop derivation of the Wilson polygon - MHV amplitude duality*, J. Phys. A **42** (2009) 355214 [0904.0381[hep-th]].

[23] A. Gorsky and A. Zhiboedov, *Aspects of the $\mathcal{N} = 4$ SYM amplitude – Wilson polygon duality*, Nucl. Phys. B **835** (2010) 343 [0911.3626[hep-th]].

[24] J. B. Tausk, *Non-planar massless two-loop Feynman diagrams with four on-shell legs*, Phys. Lett. B **469** (1999) 225 [hep-ph/9909506].

[25] G. Kramer and B. Lampe, *Integrals for two loop calculations in massless QCD*, J. Math. Phys. **28** (1987) 945.

[26] E. E. Boos, A. I. Davydychev, *A Method Of The Evaluation Of The Vertex Type Feynman Integrals*, Moscow Univ. Phys. Bull. **42N3** (1987) 6-10.

[27] A. I. Davydychev, *Recursive algorithm of evaluating vertex type Feynman integrals*, J. Phys. A **A25** (1992) 5587-5596.

[28] C. Anastasiou, E. W. N. Glover and C. Oleari, *Scalar One-loop integrals using the negative-dimension approach*, Nucl. Phys. B **572**, 307 (2000) [hep-ph/9907494].

[29] C. Anastasiou, E. W. N. Glover and C. Oleari, *Application of the negative-dimension approach to massless scalar box integrals*, Nucl. Phys. B **565**, 445 (2000) [hep-ph/9907523].

[30] T. Binoth and G. Heinrich, *An automatized algorithm to compute infrared divergent multi-loop integrals*, Nucl. Phys. B **585** (2000) 741 [hep-ph/0004013].

[31] C. Anastasiou, F. Herzog, A. Lazopoulos, *On the factorization of overlapping singularities at NNLO*, 1011.4867[hep-ph].